Effect of Adding Sb on Microstructure, Mechanical Properties and *in Vitro* Degradation Behavior of as Cast Mg-4wt% Zn Alloy for Medical Application

Hadeer I. Mohamed[1,2]*, Mohamed E. Moussa[3], Mohamed A. Waly[3], Gamilla S. Al-Ganainy[4], Aya B. Ahmed[1], Mona S. Talaat[1]

[1]Biophysics Group, Physics Department, Faculty of Science, Ain Shams University, Cairo, Egypt
[2]Department of Neuroscience Technology, College of Applied Medical Sciences in Jubail, Imam Abdulrahman Bin Faisal University, Jubail, Kingdom of Saudi Arabia
[3]Department of Manufacturing Technology, Laboratory of Foundry, Central Metallurgical Research and Development Institute (CMRDI), Helwan, Egypt
[4]Physics Department, Faculty of Science, Ain Shams University, Cairo, Egypt
Email: *hiibrahim@uod.edu.sa

Abstract

Magnesium (Mg) and its alloys are one of a novel kind of biodegradable metallic implants which attracted much fundamental research to develop its clinical application. Nevertheless, it has more restrictions in biomedical applications because it degrades too fast at the early stage after implantation, thus commonly leading to some problems such as early fast mechanical loss, hydric bubble aggregation, gap formation between the implants and the tissue. This work aims to study the effect of 0.5 wt% Sb addition on the microstructure, mechanical properties and degradation behavior of as cast Mg-4wt% Zn alloy. The evaluation process was conducted using optical and scanning electron microscopy, X-ray diffraction, tensile and compression tests, in addition to a corrosion study by immersing in simulated body fluid (SBF). Results showed that Sb refines the grain size of the base alloy and also enhances its mechanical properties and degradation rate as well. These were due to the formation of the secondary phase of Mg_3Sb_2. To get better degradation rate, the Mg-4wt% Zn and Mg-4wt% Zn-0.5wt% Sb alloys are coated with Ca-P using autocatalytic technique. The results demonstrated that the formed coat layer improves the degradation rate of samples under the condition of this study. The current study shows that Mg-4wt% Zn-0.5wt% Sb alloy has good mechanical properties and when it coated by Ca-P, it gave a better corrosion resistance that makes it ideal for biodegradable medical application.

Graphical Abstract
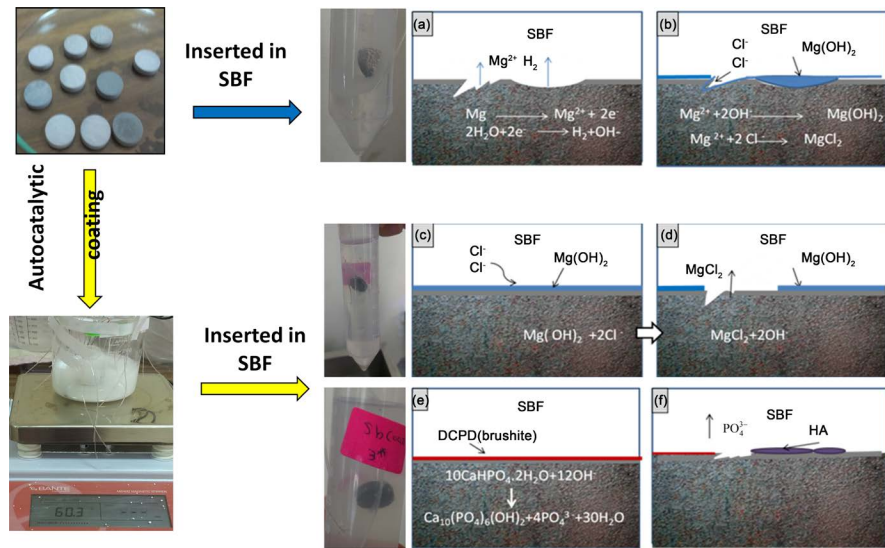
Keywords

Mg Alloy, Mechanical Properties, Autocatalytic Route, Degradation Rate, Calcium Phosphate Coating

1. Introduction

Recently biodegradable metallic implants have notable consideration in biomaterial field. Their degradation after a certain time, leads to reduce the call for extra surgery to remove the short-term implant. Mg alloy has a great interest as a biodegradable implant because its biocompatibility as it found naturally in bone; it can directly influence bone-resorbing cells and consider as a vital factor for bone metabolism. Many clinical *in vivo* and *in vitro* studies have been recommended Mg-base implants due to their good biocompatibility and their mechanical properties comparable with those of natural bone [1] [2]. The Mg density is (1.7 - 2.0 g/cm^3) which is a slightly lower than that of natural bone (1.8 - 2.1 g/cm^3), and its elastic modulus (41 - 45 GPa) is closer to those of the human bone (10 - 40 GPa) [3]. All these properties reduce the probability of stress shielding effect observed in the case of higher modulus materials such as titanium alloys [4]. Unfortunately, the application of magnesium as an implant has some restrictions such as its high degradation rate, especially in an aggressive chloride medium like a human body. This implant may degrade and reduce its mechanical properties before new tissues are completely healed [5]. Hence element alloying and surface modification are effective methods to improve rapid degradation of Mg and also to enhance their mechanical properties besides aiding in decrease corrosion.

Many elements such as Ca, Mn, Al, Zn, Si, and Sr are used as alloying ele-

ments with magnesium. In the present research, zinc (Zn) and antimony (Sb) were chosen as alloying elements. Zn is a commonly used as alloying element with magnesium and its strengthening effect is only following aluminum. It furthermore assists to eliminate the harmful effect of impurities such as iron and nickel, thus improving the corrosion resistance of magnesium alloys [6]. Also, 4wt% Zn which was chosen in this work was reported to be the optimum Zn content for tensile and mechanical strengthening over the range of alloying [7]. Moreover, zinc is vital for many biological functions, plays a fundamental role in the metabolic activities of the body's enzymes, essential for cell division and the creation of protein and DNA. Whereas excessive exposure toxicity of Zn is rare, Zn shortage has a harmful effect on growth, neuronal development, and immunity [4]. On the other hand, it is reported that the addition of 0.4 wt% Sb gives high mechanical properties, however, at the higher Sb level of 0.7 wt% the strength and hardness decrease [8]. Therefore, in present work, 0.5 wt% Sb is added to Mg-4wt% Zn alloy to study its effect on mechanical properties and degradation behavior. On the other hand the biological effect of Sb still needs more experimental research.

To improve corrosion resistance and biocompatibility of prepared alloys, the surface will be coated with Ca-P layer. Ca and P are the major elements in bone minerals. Thus, Ca-P coatings, especially osteoconductive minerals such as hydroxyapatite (HA) and tricalcium phosphate (TCP), should be useful in constructing new bone and promoting osteointegration around Mg implants [9]. Niu, Jialin, *et al.* [10] reported that the Ca-P coat improves the corrosion resistance of Mg-Nd-Zn-Zr alloy and reduced the hemolysis rate from 48% to 0.68%. Song, Yang, *et al.* [9] showed that both the HA and FHA (fluoridated hydroxyapatite) coating could promote the nucleation of osteoconductive minerals (bone-like apatite or β-TCP), while the precipitates on the uncoated Mg-Zn alloy in modified simulated biological fluid had low Ca/P molar ratios, which delayed bone-like apatite formation.

Several coating techniques have been investigated, but due to the special properties of Mg as high reactivity and relatively low melting point (650˚C), not all coating procedures can be suitable for Mg [11]. Seeing that the biomimetic coating would be helpful in coating biodegradable substrates such as Mg-alloys, it reduces the incubation times in SBF during the coating procedure [12]. As reported this resulted in the formation of non-uniform and porous Ca-P coating on Mg substrates [13], in addition to hydrogen bubbles formed on the Mg surface during immersion. When using a Sol gel technique for Mg substrates, the temperatures should be less than the melting point of pure Mg (650˚C) [14] to avoid affecting the surface integrity of the Mg substrate. Accordingly, in the present work autocatalytic technique which reported in previous studies [15] [16] [17] is used. This technique is simple, economical, does not require high temperature and setup in short time which minimize the chance of degradation.

So as there is little information on Mg-Zn-Sb, as biodegradable implant, the

present work aims to study the effect of Sb addition on microstructure, mechanical and degradation behavior of Mg-4wt% Zn alloy. Also, we intend to study the effect of the autocatalytic technique on degradation to get an appropriate alloy for load bearing medical applications.

2. Material and Methods

2.1. Material Preparation

The base composition of the studied alloy was Mg-4wt% Zn. 0.5 wt% Sb was added to the base alloy in order to investigate its effect on microstructure, mechanical properties and the degradation rate. The alloy was prepared from commercial pure Mg (99.8 wt% purity), Zn (99.98 wt% purity), and Sb (99.99 wt% purity). Before melting process a charge calculations are performed and with respect to experience, the 90% efficiency of melting process and 10% losses during melting can be estimated and be in consideration. After that melting the charge of about 1.5 kg of each alloy in a graphite crucible placed in an electric resistance furnace. The melting and pouring processes were carried out under gas mix consists of tetrafluoroethane (CF_3CH_2F, HFC-134a, 1 vol.%) and carbon dioxide (CO_2, Bal.). Firstly, commercial Mg ingots were melted to above 650°C, and then Zn with melting point 419°C was added into Mg melt. After that, the melt were heated to about 720°C, and then Sb with melting point 630°C was added into Mg melt. The melt was manually stirred for 3 min using a stainless steel rod, and then was held for additional 15 min in order to get full homogenization. Before pouring the melt, test sample of the melt is required to make a chemical analysis correction using X-ray fluorescence (XRF) analyzer. Depending on the test result a correction process is required either by diluting (adding pure Mg) or concentrating (adding alloying element as Sb or Zn or both) to get the required alloy composition. After that, the slag was removed, and then the melt was poured at about 720°C into a preheated cast iron mold up to 100°C with dimensions of outer diameter (100 mm), inner diameter (50 mm) and length (250 mm). The chemical compositions of the prepared alloy were determined by using X-ray fluorescence (model Axios advanced-PANALYTCAL, The Netherlands).

2.2. Microstructure Characterization

All metallographic specimens were cut at the same position of 10 mm from the bottom of castings. Grinding of the specimens were carried out on wet SiC papers, down to grit size 1200 then followed by fine polishing with diamond, particle size from 1 to 6 μm, on nylon cloth, rinsing with water and ethyl alcohol. For best results, the polished surface must be mirror like, *i.e.*, free from any residual layer. After that, the specimens are etched by solution with 10 ml nitric acid, 30 ml acetic acid, 40 ml water, and 120 ml ethanol for 2 - 3 min [18].

The microstructures of the specimens were analyzed by optical microscope (OM) (Zeis model Axiotech, Germany). Six OM micrographs were taken for each sample from the observed area at a magnification of 100×. The average

grain size of α-Mg was measured by using an image analyzer. All α-Mg grains existed in one picture taken from the observed area were measured.

Phase constituents of samples were analyzed by X-ray diffraction (XRD) (model X'PERT PRO, The Netherlands) using Cu-Kα (K = 1.54056Å) radiation in step scan of 2θ from 20° to 80° with an increment of 0.02° and a scanning speed of 4°/min. Scanning electron microscope (Inspect S50.Fel, The Netherlands) equipped with an energy dispersive X-ray spectrometer (EDS) were used to conduct microstructure analysis.

2.3. Mechanical Tests

Tensile and compression tests were carried out using LFM-L-20KN Computer controlled and digital display electromechanical universal testing machine (model LFM-L-20KN (bench top), Switzerland). The dimensions of a cylindrical tensile specimen are shown in **Figure 1** according to ASTM E8M [19]. Three specimens were tested with a strain rate of 0.1 mm/min for each alloy. Cylindrical samples with a diameter of 10 mm and a height of 8 mm were used for the compression test.

2.4. Sample Coating

2.4.1. Pre-Treatment
Before coating, samples were cut into discs (10 mm diameter and 2 mm thickness). Each sample was cleaned with acetone, 70% ethanol, and finally distilled water for 15 min each, in an ultrasonic cleaner. Then samples were etched in Kroll's reagents for 10 min at 20°C next washed with distilled water to remove the native oxide surface. Afterward, samples were immersed in 10 M NaOH bath at 60°C for 24 h followed by heating and holding at 100°C for 1 h [15] [16] [17].

2.4.2. Coating by Autocatalytic Bath
After the pretreatment step, samples were immersed in an acidic autocatalytic bath under magnetic stirrer for 2 h at 60°C ± 2°C at pH 5 to get different phases Ca-P coatings on samples. The composition of acidic bath was reported in previous work [15] [16] [17].

2.4.3. Characterization of Coating
Surface morphology and the chemical compositions of the deposited layer were analyzed by field emission scanning electron microscope (Quanta 250) with EDS. Structure of coated layer was analyzed by X-ray diffraction (XRD) with similar condition used for microstructure composition.
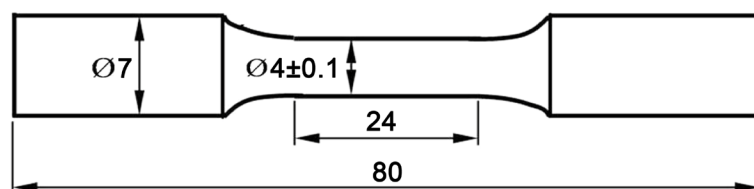

Figure 1. Dimensions of the tensile specimen (mm) [19].

2.5. Corrosion Evaluation by Immersion in Simulated Body Fluid (SBF)

Corrosion resistance by *in vitro* degradation method was obtained by weight loss measurements which were performed by immersing the alloy samples in SBF. The chemical composition of c-SBF in comparison to human blood plasma was reported in several studies [20]. The pH value of the initial solution was adjusted to 7.4. The whole test cell was maintained at 37°C ± 1°C in a shaking water bath to prevent aggregation of the precipitates on sample surfaces [15]. In this test two categories of samples (non-coated (bare), coated) were studied. The samples were immersed for 14 days in SBF solution with refreshment after 3 days. The refreshment was done to simulate the metabolic environment of the human body and study the formed layer. The appearance and microstructure of the specimens were characterized by SEM with EDS. The pH value of the solution was measured by a pH meter with an accuracy of ±0.01.

The sample weight was measured every 24 hours of immersion after removal of corrosion products with a chromic acid. The degradation rates were calculated by the following equation according to the standard:

$$DR = \frac{\Delta m}{AT\rho} \qquad (1) \quad [21]$$

where: DR is the degradation rate (mm/hr), Δm is the mass loss (g), A is the initial surface area exposed to the SBF (mm^2), T is the immersion time (hr), and ρ is the density of tested sample (g/mm^3).

The concentrations of Ca and P ions in SBF after immersion of coated Mg-4wt% Zn and Mg-4wt% Zn-0.5wt% Sb for 14 days were measured using a UV-Vis spectrophotometer and the specific kits (Biodiagnostic, Diagnostic and research reagents, Egypt) at wavelength 640 nm, 585 nm for phosphorus and calcium respectively.

3. Results

3.1. Chemical Composition

The chemical compositions of the prepared alloy were determined using X-ray fluorescence (XRF) analyzer. Table 1 showed the obtained chemical composition of the investigated alloys.

3.2. Phases and Microstructure Characterization

Figure 2 shows the XRD results and the optical microstructure of the as-cast prepared alloys. As shown in Figure 2(a), *α*-Mg and MgZn phases are the only

Table 1. The chemical composition of the prepared alloys (wt%).

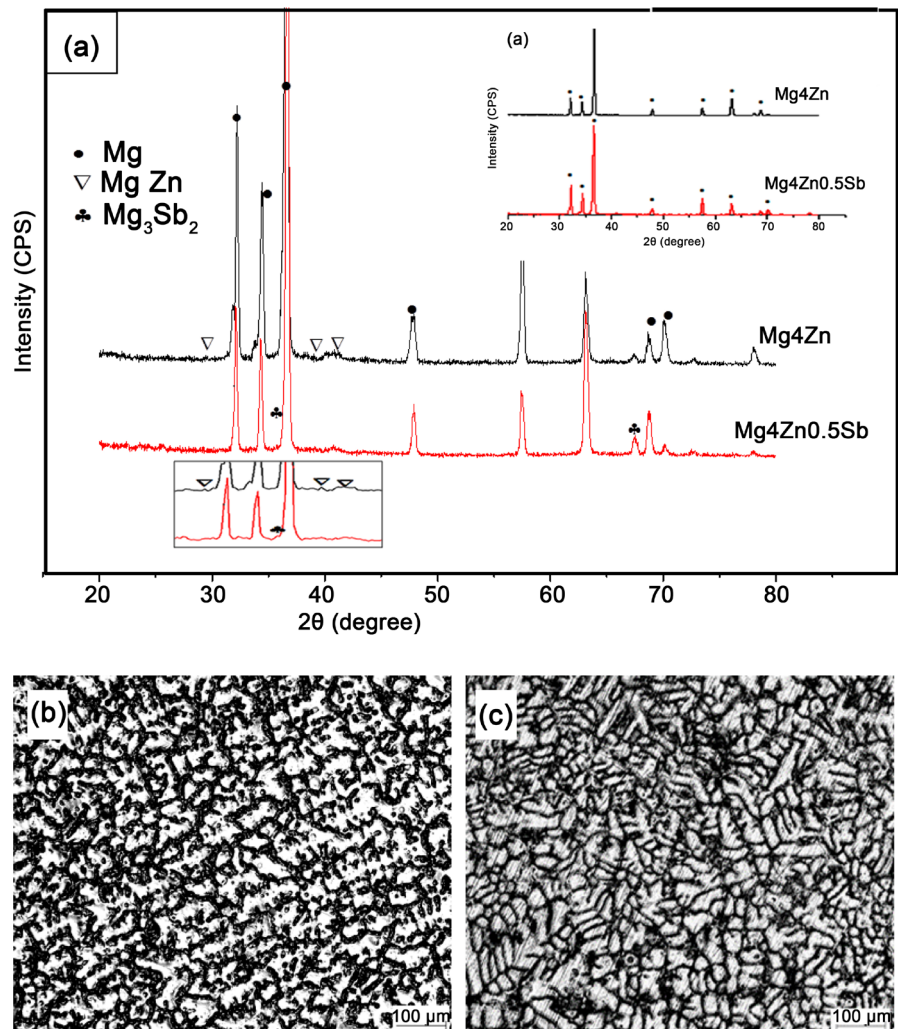| Prepared alloy	Mg	Zn	Sb	Fe	Cu
Mg-4Zn	96.012	3.95	-	0.007	0.031
Mg-4Zn-0.5Sb	95.575	3.91	0.466	0.016	0.033

Figure 2. (a) XRD patterns of as-cast alloys Mg-4wt% Zn and Mg-4wt% Zn-0.5wt% Sb, optical micrographs of as-cast alloys (b) Mg-4wt% Zn and (c) Mg-4wt% Zn-0.5wt% Sb.

constituents of the Mg-4wt% Zn alloy. These two phases have also been reported to exist in the as-cast microstructure of an Mg-4wt% Zn alloy [22]. In the Sb containing materials, however, some new peaks corresponding to the Mg_3Sb_2 intermetallic phase appear in the patterns. **Figure 2(b)** & **Figure 2(c)** show that the coarse dendritic structure of the Mg-4wt% Zn alloy is generally refined from about 100 μm (**Figure 2(b)**) to about 53 μm after the addition of 0.5 wt% Sb (**Figure 2(c)**).

For clear observations of the constitutive phases, SEM micrographs with EDS and elemental mapping of Mg, Zn and Sb of investigated alloys are shown in **Figure 3** & **Figure 4**, respectively. **Figure 3(a)** shows the microstructure of the Mg-4wt% Zn alloy which consists of the primary α-Mg matrix (region A), while the second phase appears as white island-like (region B) which was identified by EDS to be composed of Mg and Zn elements. Combined with the XRD results shown in **Figure 2(a)**, it is found that the island-like particles are most likely the MgZn particles and thus the lamellar eutectic structure consists of α-Mg +
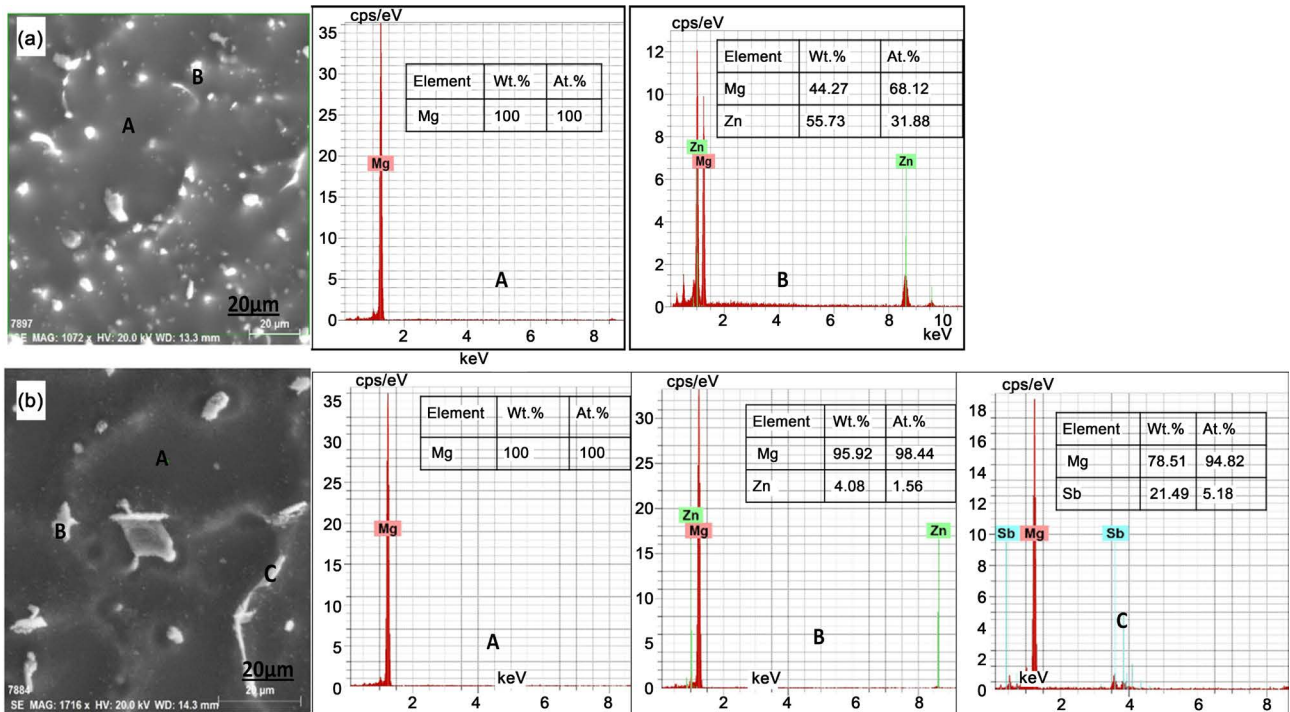
Figure 3. SEM micrographs with EDS showing intermetallic phases in as-cast alloys (a) Mg-4wt% Zn and (b) Mg-4wt% Zn-0.5wt% Sb.
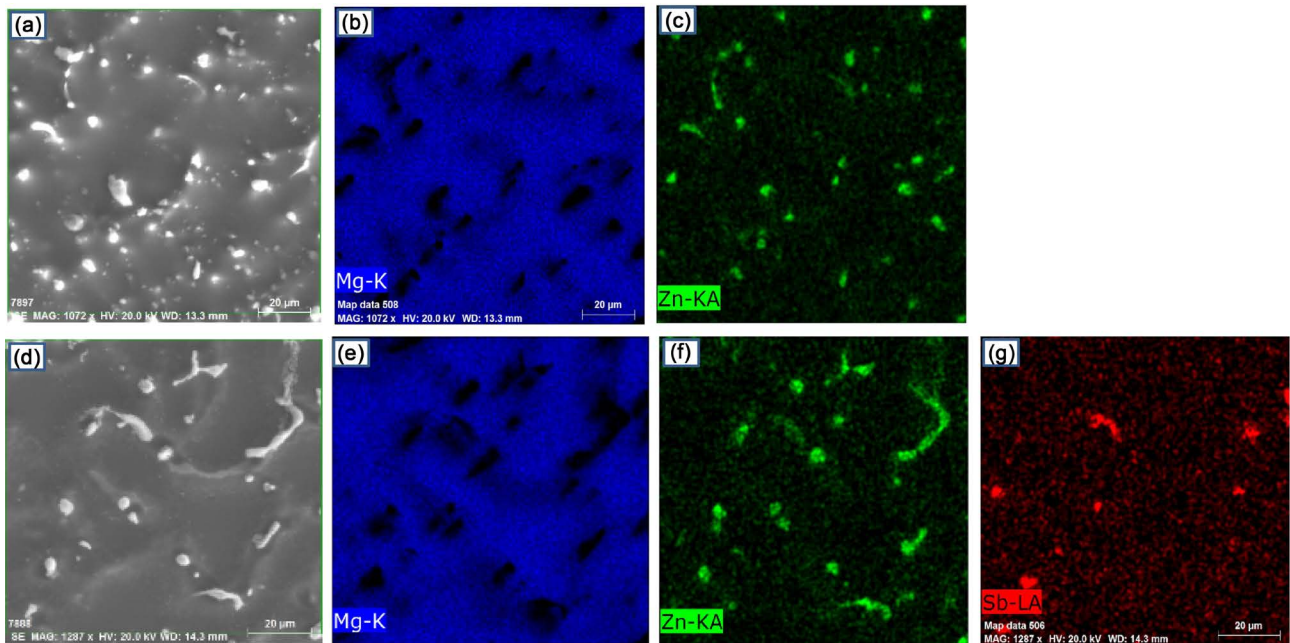

Figure 4. (a) SEM micrograph and EDS elemental mapping of (b) Mg and (c) Zn in as-cast alloy Mg-4wt% Zn and (d) SEM micrograph and EDS elemental mapping of (e) Mg, (f) Zn and (g) Sb in as-cast alloy Mg-4wt% Zn-0.5wt% Sb.

MgZn. In Sb-added alloy (**Figure 3(b)**), a new rod shape particles contain Mg and Sb is appeared (region C) which was detected by XRD as Mg_3Sb_2 (**Figure 2(a)**).

Figure 4 shows EDS elemental mapping of Mg, Zn and Sb in the investigated

alloys. It can be seen that the non-uniform distribution of Zn (**Figure 4(c)**) in the interdendritic regions of *α*-Mg (**Figure 4(b)**). With addition of 0.5 wt% Sb, the distribution of Sb is mostly at the boundaries of the *α*-Mg dendrites (**Figure 4(g)**) and the uniform distribution of Zn at dendrites boundaries (**Figure 4(f)**).

3.3. Mechanical Properties

The ultimate tensile strength, elongation and Compressive strength of investigated alloys, are summarized in **Table 2**.

3.4. Characterization of Coating

It is observable that autocatalytic bath changes the morphologies of the based alloys as shown in **Figure 5**. Homogeneous coating was observed for both alloys. At higher magnification it was found that bulk coating was formed after immersion of Mg-4wt% Zn in the bath with distribution of white grain on its surface (**Figure 5(b)**). EDS analysis of this layer demonstrates the presence of Mg, O

Table 2. The ultimate tensile strength, elongation and Compressive strength of investigated alloys.

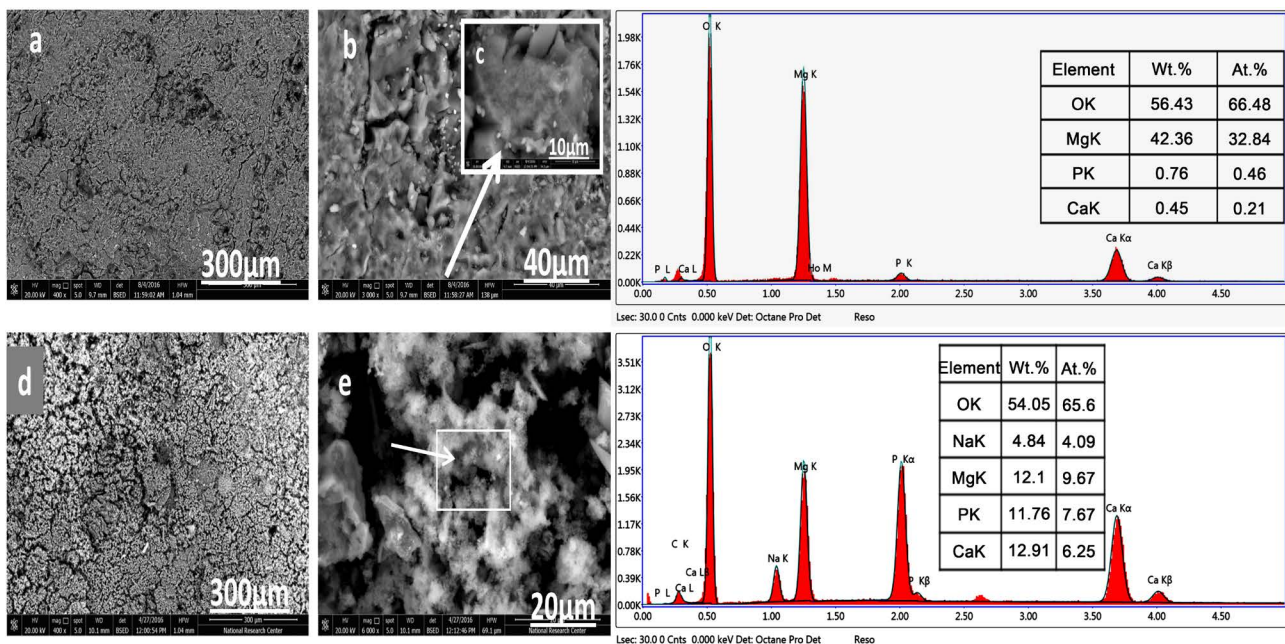| Material	Ultimate tensile strength, MPa	Elongation%	Compressive strength, MPa
Cortical bone [28]	135	1.07 - 2.10	164 - 240
Pure Mg [29]	97	7	185.4
Mg-4Zn	100.70	8	222.5
Mg-4Zn-0.5Sb	185	6.88	268.5

Figure 5. SEM micrographs with EDS showing the coat formed on the surface of Mg-4wt% Zn ((a)-(c)), Mg-4wt% Zn-0.5wt% Sb ((d), (e)).

with traces of phosphorus and calcium on the surface of the alloy (**Figure 5(c)**). While after addition of Sb, an agglomerate of fine grains covers the surface of the alloys (**Figure 5(e)**). EDS of this layer consist of higher amount of Ca, P in addition to Na ions. The addition of Sb allows the precipitation of Ca-P layer as a nucleation for hydroxyapatite (HA). The atomic calcium phosphate ratio $n(Ca)/n(P)$ value suggest that formed layer may be dicalcium Phosphate dihydrate (DCPD), also known as brushite which act as a precursor phase.

The XRD patterns Mg-4wt% Zn and Mg-4wt% Zn-0.5wt% Sb alloys after coating (**Figure 6**) show existence of $Mg(OH)_2$ peaks which confirmed by SEM results. It is noted that Mg-4wt% Zn displays high intensity of $Mg(OH)_2$ peaks compared with Mg-4wt% Zn-0.5wt% Sb.

Other than brushite phase cannot be detected by XRD as it is very thin and non uniform layer. Improvement of the formed layer will be considered in future work by increasing the immersion time and pH of autocatalytic bath.

3.5. Corrosion Evaluation by Immersion in Simulated Medium

The average mass loss and the rate of degradation of Mg-4wt% Zn and Mg-4wt% Zn-0.5wt% Sb alloys before and after coating during 14 days of immersion in SBF are illustrated in **Figure 7**.

The change in mass is an indicator for the degradation of the alloy samples. **Figure 7** illustrates that, the coated sample of Mg-4Zn showed the lowest rate of degradation in the first 24 hr of immersion. As the sample has a porous, and
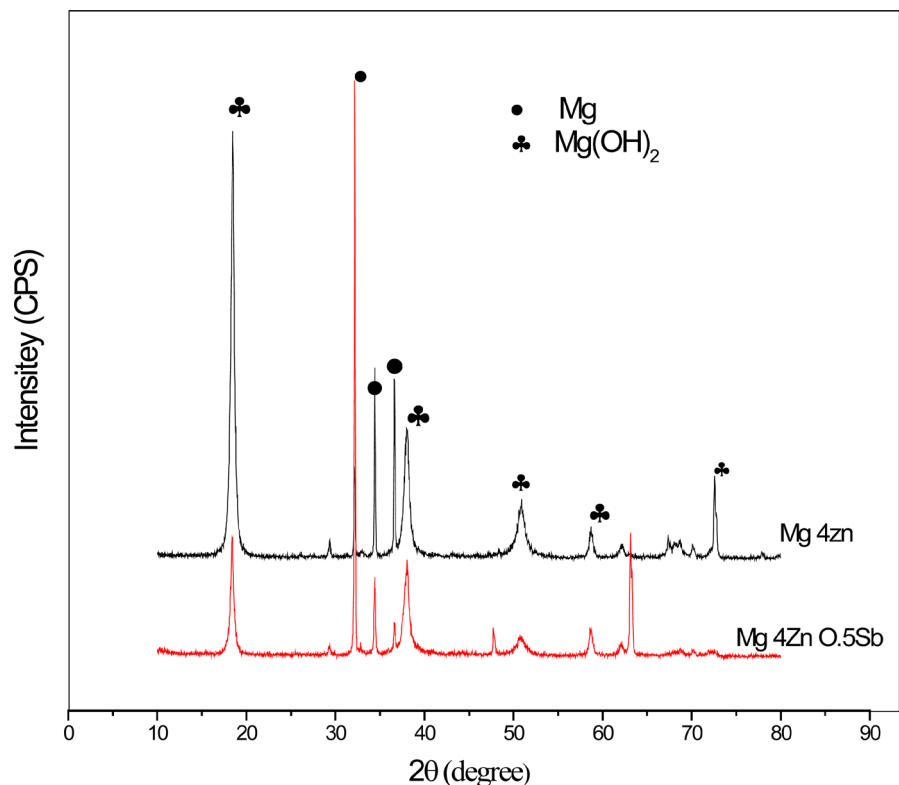

Figure 6. XRD patterns of Mg-4wt% Zn and Mg-4wt% Zn-0.5wt% Sb samples after coating.
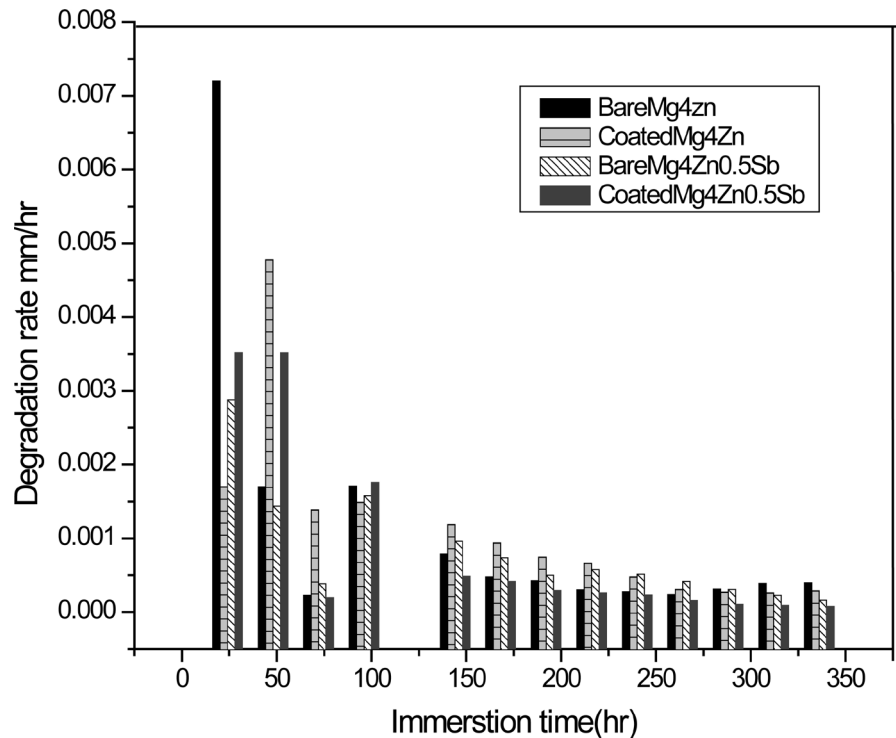
Figure 7. The degradation rate during immersion of coated and bare alloys of Mg-4Zn and Mg-4Zn-0.5Sb.

dense layer of Mg(OH)$_2$, which can reduce the corrosion rate. However, more than 48 hr of immersion, the degradation rate of both coated samples increased. As the protective Mg(OH)$_2$ layer converted into a more soluble MgCl$_2$. This will cause the coated Mg-4Zn alloys to expose to the solution and stimulate the degradation. As well, the coated Mg-4Zn-0.5Sb sample displayed high rate of degradation due to dissolving of brushite coat. On the other hand, the degradation rate of the bare samples of Mg-4Zn and Mg-4Zn-0.5Sb decreased due to formation of Mg(OH)$_2$ protective layer.

By refreshing the solution after 3 days of immersion, it is found that, the degradation rate increased again for all the samples. This caused by Cl$^-$ ions which accelerate the electrochemical reaction rate from magnesium and leads to more degradation of the Mg matrix. Seeing that the exposure period continues, the corrosion rate reached a steady state as the rate of formation of Mg(OH)$_2$ is equal to destruction of it by MgCl$_2$. At the end of immersion time it is observed that the Mg-4Zn-0.5Sb samples shows the lowest rate of degradation specially the coated one.

Figure 8 shows the micrograph of the surface of Mg-4Zn and Mg-4Zn-0.5Sb alloys after immersion in the SBF solution for 336 h. Figure 8(a), Figure 8(d), Figure 8(g), and Figure 8(j)) show the surface cracks which formed from dehydration of the surface layer in the air [23]. Existence of cracks accelerates corrosion of the substrate by making solution come into contact with the matrix [24]. The bare Mg-4Zn alloy and Mg-4Zn-0.5Sb (Figure 8(a), Figure 8(g)) showed deeper
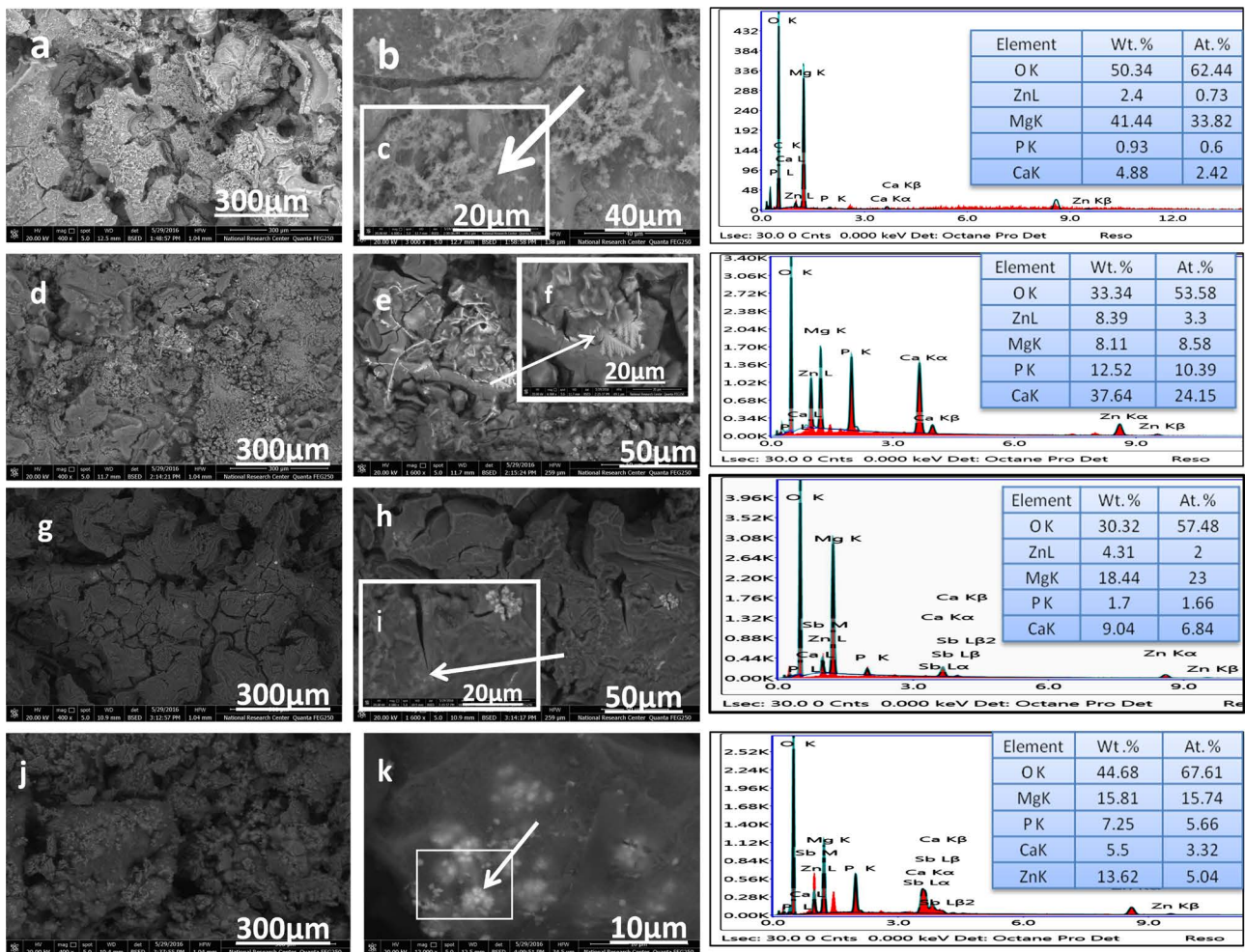
Figure 8. SEM micrographs of samples surface after SBF immersion. ((a)-(c)) bare Mg-4Zn, ((d)-(f)) coated Mg-4Zn, ((g)-(i)) bare Mg-4Zn-0.5Sb, ((j), (k)) coated Mg-4Zn-0.5Sb.

Element	Wt.%	At.%
O K	50.34	62.44
ZnL	2.4	0.73
MgK	41.44	33.82
P K	0.93	0.6
CaK	4.88	2.42

Element	Wt.%	At.%
O K	33.34	53.58
ZnL	8.39	3.3
MgK	8.11	8.58
P K	12.52	10.39
CaK	37.64	24.15

Element	Wt.%	At.%
O K	30.32	57.48
ZnL	4.31	2
MgK	18.44	23
P K	1.7	1.66
CaK	9.04	6.84

Element	Wt.%	At.%
O K	44.68	67.61
MgK	15.81	15.74
P K	7.25	5.66
CaK	5.5	3.32
ZnK	13.62	5.04

and thicker cracks than coated alloys (**Figure 8(d)**, **Figure 8(j)**). The EDS analysis showed the presence of $Mg(OH)_2$ consistent with the atomic ratio of Mg to O (1:2) on the surface of bare Mg-4Zn (**Figure 8(c)**). The EDS results of the corroded layer on coated samples (**Figure 8(f)**, **Figure 8(k)**) showed the existence of Mg and O as well as amounts of Ca and P, which represents formation of HA. As observed in EDS results that the bare samples have trace amounts of Ca and P in compare with the coated samples.

This consequence points that the coated samples are more successful to form nucleation of Ca-P which initiates the formation of HA. To confirm that, the concentrations of Ca and P ions in SBF after immersion of coated Mg-4Zn and Mg-4Zn-0.5Sb for 14 days are measured as presented in **Figure 9**.

4. Discussion

It is illustrious that the difference in the electronegativity values between Mg of 1.31, Zn of 1.6 and Sb of 2.05, provides the Sb more tendencies to form a compound with Mg than with Zn [8] [25]. Therefore, all of the Sb added to Mg-4wt%
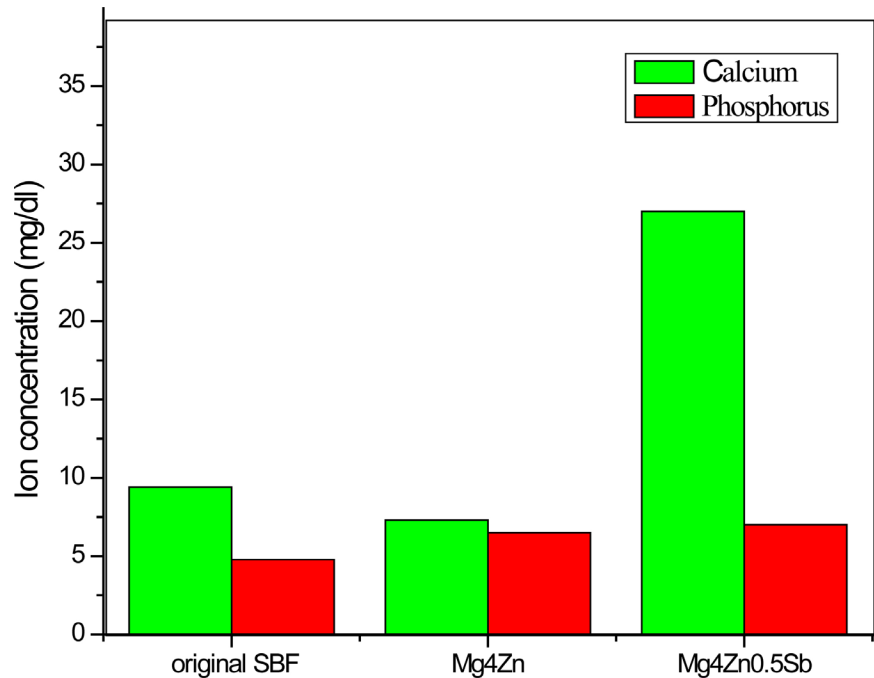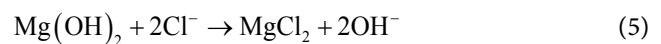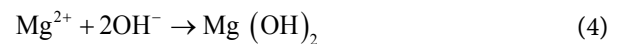
Figure 9. Concentrations of Ca and P ions in SBF after immersion of coated alloy samples for 14 days.

Zn alloy, is consumed to form Mg_3Sb_2 particles [8]. The refining effect of Sb in cast magnesium alloys has attracted some attention [26] [27] [28]. It has been reported that small additions of Sb had a great effect on the microstructural refinement and mechanical properties of the cast Mg-5%Sn alloy. Adding Sb to ZA84 [27] and AZ91 [26] has also resulted in microstructural refinement and improved room and high-temperature mechanical properties. Based on the SEM observations (**Figure 4(d)**, **Figure 4(g)**), where no Mg_3Sb_2 compound is detected inside the Mg grains and all particles are found to be formed inside the inter-dendritic spaces. Therefore, the segregation of Mg_3Sb_2 particles at the liquid/solid interface would restrict the growth of a-Mg dendrites during solidification and thus refine the structure. These results are also confirmed by the previous work reported by R. Alizadeh *et al.* [8]. Also the addition of 0.5 wt% Sb could improve the mechanical properties of Mg-4wt% Zn alloy. Owing to the relation of mechanical properties with the microstructure of the investigated alloys, the improved mechanical properties of the Sb-added alloy outcome from their microstructures. It is well known that the fine microstructure is usually beneficial to tensile properties of engineering alloys. According to Griffith's theory [29], the fracture stress of a material increases with decreasing grain size, in inverse proportion to the square root of the grain size. As shown before, the addition of Sb into the base Mg-4wt% Zn alloy cause grain refinement. Therefore, that leads to improve mechanical properties of the as-cast Sb-added alloys which is bio-compatible with mechanical properties of cortical bone [30] in comparison with the base alloy and pure Mg [24]. It's clear that the addition of Sb leads to delay the loss of the mechanical properties of the binary Mg-4wt% Zn alloy during

implantation

For a closer explanation, in the early stage of an immersion, Mg matrix of bare samples dissolved and transformed into the stable Mg^{2+} ion (Equations ((2), (3))). This dissolution of Mg is associated with release H_2 bubbles observed after immersion and OH^- ions which lead to the increase pH of SBF [31]. After that, a protective layer of $Mg(OH)_2$ is formed (Equation (4)) and prevent solution from direct contact with the substrate. This leads to reduce the degradation rate for a while. However, the aggressive Cl^- ions in the medium attack the thin film of $Mg(OH)_2$ and convert it into a more soluble $MgCl_2$ (Equation (5)). So the substrate of the bare samples becomes in contact with the solution again [32].

$$Mg \rightarrow Mg^{2+} + 2e^- \tag{2}$$

$$2H_2O + 2e^- \rightarrow H_2 + 2OH^- \tag{3}$$

$$Mg^{2+} + 2OH^- \rightarrow Mg(OH)_2 \tag{4}$$

$$Mg(OH)_2 + 2Cl^- \rightarrow MgCl_2 + 2OH^- \tag{5}$$

Equations (2)-(5) [24]

The coated Mg-4Zn sample which has a dense protective layer of $Mg(OH)_2$. This layer protects the sample from degradation at first, but after that the Cl^- ions dissolve it into $MgCl_2$ according to (Equation (5)). In case of coated Mg-4Zn-0.5Sb, the brushite (DCPD) layer is unstable and soluble in SBF especially with increasing pH value. Also brushite convert into HA [33] [34] and form layer against corrosion (Equation (6)).

$$10CaHPO_4 \cdot 2H_2O + 12OH^- \rightarrow Ca_{10}(PO_4)_6(OH)_2 + 4PO_4^{3-} + 30H_2O \quad (6) \ [9]$$

As shown in **Figure 9** the increase of Ca and P ion concentrations after immersion is due to partially dissolve of the coated layer within the corrosion. Fortunately the presence of the Ca and P ion, and also the increasing of pH during immersion can encourage HA nucleation. So finally it remarks that the formation of the hydroxyapatite in the SBF is self-generated after a certain period of immersion. The formation of HA not only decrease the degradation rate, but it is also reported that during implantation, the living bone will bond through this apatite layer formed on the surface of implant so the coating step is very helpful.

5. Conclusions

In this article, the as-cast Mg-4wt% Zn and Mg-4wt% Zn-0.5wt% Sb alloys were investigated as degradable metallic implants. The alloys are mainly composed of the matrix α-Mg and MgZn as secondary phase. The addition of Sb refines the grain size and improves mechanical properties due to the formation of the secondary phase of Mg_3Sb_2.

Immersion result showed that the Ca-P treatment provides a protective layer that improves the corrosion resistance. The degradation rate measured at the end of immersion time improved from 3.5 mm/yr, 2.5 mm/yr for bare and coated Mg-4Zn respectively to 1.4 mm/yr, 0.7 mm/yr for bare and coated Sb-added alloy

respectively. So it is clear that the addition of Sb and coating procedure are very effective steps to enhance degradation behavior.

References

[1] Gu, X., Zheng, Y., Cheng, Y., Zhong, S. and Xi, T. (2009) *In vitro* Corrosion and Biocompatibility of Binary Magnesium Alloys. *Biomaterials*, **30**, 484-498. https://doi.org/10.1016/j.biomaterials.2008.10.021

[2] Witte, F., Kaese, V., Haferkamp, H., Switzer, E., Meyer-Lindenberg, A., Wirth, C. and Windhagen, H. (2005) *In vivo* Corrosion of Four Magnesium Alloys and the Associated Bone Response. *Biomaterials*, **26**, 3557-3563. https://doi.org/10.1016/j.biomaterials.2004.09.049

[3] Song, G. (2007) Control of Biodegradation of Biocompatable Magnesium Alloys. *Corrosion Science*, **49**, 1696-1701. https://doi.org/10.1016/j.corsci.2007.01.001

[4] Salleh, E.M., Ramakrishnan, S. and Hussain, Z. (2016) Synthesis of Biodegradable Mg-Zn Alloy by Mechanical Alloying: Effect of Milling Time. *Procedia Chemistry*, **19**, 525-530. https://doi.org/10.1016/j.proche.2016.03.048

[5] Zhou, P. and Gong, H. (2012) Phase Stability, Mechanical Property, and Electronic Structure of an Mg-Ca System. *Journal of the Mechanical Behavior of Biomedical Materials*, **8**, 154-164. https://doi.org/10.1016/j.jmbbm.2011.12.001

[6] Huan, Z., Leeflang, M., Zhou, J., Fratila-Apachitei, L. and Duszczyk, J. (2010) *In vitro* Degradation Behavior and Cytocompatibility of Mg-Zn-Zr Alloys. *Journal of Materials Science: Materials in Medicine*, **21**, 2623-2635. https://doi.org/10.1007/s10856-010-4111-8

[7] Boehlert, C. and Knittel, K. (2006) The Microstructure, Tensile Properties, and Creep Behavior of Mg-Zn Alloys Containing 0-4.4 wt% Zn. *Materials Science and Engineering A*, **417**, 315-321. https://doi.org/10.1016/j.msea.2005.11.006

[8] Alizadeh, R. and Mahmudi, R. (2010) Effect of Sb Additions on the Microstructural Stability and Mechanical Properties of Cast Mg-4Zn Alloy. *Materials Science and Engineering A*, **527**, 5312-5317. https://doi.org/10.1016/j.msea.2010.05.029

[9] Song, Y., Zhang, S., Li, J., Zhao, C. and Zhang, X. (2010) Electrodeposition of Ca-P Coatings on Biodegradable Mg Alloy: *in vitro* Biomineralization Behavior. *ActaBiomaterialia*, **6**, 1736-1742. https://doi.org/10.1016/j.actbio.2009.12.020

[10] Niu, J., Yuan, G., Liao, Y., Mao, L., Zhang, J., Wang, Y., *et al.* (2013) Enhanced Biocorrosion Resistance and Biocompatibility of Degradable Mg-Nd-Zn-Zr Alloy by Brushite Coating. *Materials Science and Engineering C*, **33**, 4833-4841. https://doi.org/10.1016/j.msec.2013.08.008

[11] Shadanbaz, S. and Dias, G.J. (2012) Calcium Phosphate Coatings on Magnesium Alloys for Biomedical Applications: A Review. *Acta Biomaterialia*, **8**, 20-30.

[12] Chen, Y., Mak, A.F., Li, J., Wang, M. and Shum, A.W. (2005) Formation of Apatite on Poly (a-Hydroxy Acid) in an Accelerated Biomimetic Process. *Journal of Biomedical Materials Research Part B: Applied Biomaterials*, **73**, 68-76. https://doi.org/10.1002/jbm.b.30178

[13] Gray-Munro, J.E., Seguin, C. and Strong, M. (2009) Influence of Surface Modification on the *in Vitro* Corrosion Rate of Magnesium Alloy AZ31. *Journal of Biomedical Materials Research Part A*, **91**, 221-230. https://doi.org/10.1002/jbm.a.32205

[14] Phani, A., Gammel, F. and Hack, T. (2006) Structural, Mechanical and Corrosion Resistance Properties of Al_2O_3-CeO_2 Nanocomposites in Silica Matrix on Mg Alloys by a Sol-Gel Dip Coating Technique. *Surface and Coatings Technology*, **201**,

3299-3306.

[15] Mohammed, H.I., Carradò, A. and Abdel-Fattah, W.I. (2015) Noble Metals Role in Autocatalytic Phosphate Coatings on TAV Alloys. I. Ag Functionalization of Autocatalytic Phosphate Deposition on TAV Alloys. *Surface and Coatings Technology*, **282**, 171-179.

[16] Le, V.Q., Pourroy, G., Cochis, A., Rimondini, L., Abdel-Fattah, W.I., Mohammed, H.I., *et al*. (2014) Alternative Technique for Calcium Phosphate Coating on Titanium Alloy Implants. *Biomatter*, **4**, e28534. https://doi.org/10.4161/biom.28534

[17] Mohammed, H.I., Abdel-Fattah, W.I., Sallam, M.A., El-Sayed, M.E., Talaat, M.S., Faerber, J., *et al*. (2012) Calcium Phosphate Coating on Ti6Al4V by Autocatalytic Route. *Bioinspired, Biomimetic and Nanobiomaterials*, **1**, 221-228. https://doi.org/10.1680/bbn.12.00012

[18] Moussa, M.E., Waly, M.A. and El-Sheikh, A.M. (2013) Effect of High-Intensity Ultrasonic Treatment on Modification of Primary Mg2Si in the Hypereutectic Mg-Si Alloys. *Journal of Alloys and Compounds*, **577**, 693-700.

[19] Annual Book of ASTM Standards (2006) Metals-Mechanical Testing; Elevated and Low-Temperature Tests; Metallography. ASTM International, Vol. 3, Baltimore.

[20] Kokubo, T. and Takadama, H. (2006) How Useful Is SBF in Predicting *in Vivo* Bone Bioactivity? *Biomaterials*, **27**, 2907-2915.

[21] Fan, J., Qiu, X., Niu, X., Tian, Z., Sun, W., Liu, X., *et al*. (2013) Microstructure, Mechanical Properties, *in Vitro* Degradation and Cytotoxicity Evaluations of Mg-1.5 Y-1.2 Zn-0.44 Zr Alloys for Biodegradable Metallic Implants. *Materials Science and Engineering: C*, **33**, 2345-2352.

[22] Jia, H., Feng, X. and Yang, Y. (2015) Influence of Solution Treatment on Microstructure, Mechanical and Corrosion Properties of Mg-4Zn Alloy. *Journal of Magnesium and Alloys*, **3**, 247-252.

[23] Razavi, M., Fathi, M. and Meratian, M. (2010) Fabrication and Characterization of Magnesium-Fluorapatite Nanocomposite for Biomedical Applications. *Materials Characterization*, **61**, 1363-1370.

[24] Bakhsheshi-Rad, H., Idris, M., Abdul-Kadir, M., Ourdjini, A., Medraj, M., Daroonparvar, M., *et al*. (2014) Mechanical and Bio-Corrosion Properties of Quaternary Mg-Ca-Mn-Zn Alloys Compared with Binary Mg-Ca Alloys. *Materials & Design*, **53**, 283-292.

[25] Liu, Z., Chen, Z., Liu, X. and Tao, J. (2006) Influence of Antimony Addition on Heat Resistance of AE41 Magnesium Alloy. *Chinese Journal of Materials Research*, **20**, 186.

[26] Guangyin, Y., Yangshan, S. and Wenjiang, D. (2000) Effects of Sb Addition on the Microstructure and Mechanical Properties of AZ91 Magnesium Alloy. *Scripta Materialia*, **43**, 1009-1013.

[27] Balasubramani, N., Srinivasan, A., Pillai, U.S., Raghukandan, K. and Pai, B. (2008) Effect of Antimony Addition on the Microstructure and Mechanical Properties of ZA84 Magnesium Alloy. *Journal of Alloys and Compounds*, **455**, 168-173.

[28] Nayyeri, G. and Mahmudi, R. (2010) Effects of Sb Additions on the Microstructure and Impression Creep Behavior of a Cast Mg-5Sn Alloy. *Materials Science and Engineering: A*, **527**, 669-678.

[29] Cong, M., Li, Z., Liu, J. and Li, S. (2014) Effect of Sr on Microstructure, Tensile Properties and Wear Behavior of As-Cast Mg-6Zn-4Si Alloy. *Materials & Design*, **53**, 430-434.

[30] Hall, E. (1970) Yield Point Phenomena in Metals and Alloys. Macmillan, London.
https://doi.org/10.1007/978-1-4684-1860-6

[31] Zhen, Z., Xi, T.-F. and Zheng, Y.-F. (2013) A Review on *in Vitro* Corrosion Performance Test of Biodegradable Metallic Materials. *Transactions of Nonferrous Metals Society of China*, **23**, 2283-2293.

[32] Song, G., Atrens, A., St John, D., Wu, X. and Nairn, J. (1997) The Anodic Dissolution of Magnesium in Chloride and Sulphate Solutions. *Corrosion Science*, **39**, 1981-2004.

[33] Feng, Q., Cui, F., Wang, H., Kim, T. and Kim, J. (2000) Influence of Solution Conditions on Deposition of Calcium Phosphate on Titanium by NaOH-Treatment. *Journal of Crystal Growth*, **210**, 735-740.

[34] Wen, C., Guan, S., Peng, L., Ren, C., Wang, X. and Hu, Z. (2009) Characterization and Degradation Behavior of AZ31 Alloy Surface Modified by Bone-Like Hydroxyapatite for Implant Applications. *Applied Surface Science*, **255**, 6433-6438.